Growth Site Localization of Rho1 Small GTP-binding Protein and Its Involvement in Bud Formation in *Saccharomyces cerevisiae*

Wataru Yamochi,* Kazuma Tanaka,*§ Hidetaro Nonaka,*§ Akio Maeda,* Takashi Musha,* and Yoshimi Takai*‡§

*Department of Biochemistry, Kobe University School of Medicine, Kobe 650; ‡Department of Cell Physiology, National Institute for Physiological Sciences, Okazaki 444; and §Department of Molecular Biology and Biochemistry, Osaka University Medical School, Suita 565, Japan

Abstract. The Rho small GTP-binding protein family regulates various actomyosin-dependent cell functions, such as cell morphology, locomotion, cytokinesis, membrane ruffling, and smooth muscle contraction. In the yeast *Saccharomyces cerevisiae*, there is a homologue of mammalian *Rho*A, *RHO1*, which is essential for vegetative growth of yeast cells. To explore the function of the *RHO1* gene, we isolated a recessive temperature-sensitive mutation of *RHO1*, *rho1-104*. The *rho1-104* mutation caused amino acid substitutions of Asp 72 to Asn and Cys 164 to Tyr of Rholp. Strains bearing the *rho1-104* mutation accumulated tiny- or small-budded cells in which cortical actin patches were clustered to buds at the restrictive temperature. Cell lysis and cell death were also seen with the *rho1-104* mutant. Indirect immunofluorescence microscopic study demonstrated that Rholp was concentrated to the periphery of the cells where cortical actin patches were clustered, including the site of bud emergence, the tip of the growing buds, and the mother-bud neck region of cells prior to cytokinesis. Indirect immunofluorescence study with cells overexpressing *RHO1* suggested that the Rholp-binding site was saturable. A mutant Rholp with an amino acid substitution at the lipid modification site remained in the cytoplasm. These results suggest that Rho1 small GTP-binding protein binds to a specific site at the growth region of cells, where Rholp exerts its function in controlling cell growth.

THE yeast *Saccharomyces cerevisiae* grows by budding for cell division (Drubin, 1991; Nelson, 1992). This polarized cell growth is initiated by signals from the cell surface that result in realignment of the cytoskeleton and the biosynthetic machinery toward a targeting patch at the bud site. Membrane protein transport to the cell surface is mediated by vesicles, which become selectively targeted to the bud site. Bud site assembly and growth are also coupled to reorganization of the actin cytoskeleton. Disruption of the single actin gene in *S. cerevisiae* results in abnormal cell growth and intracellular accumulation of vesicles (Novick and Botstein, 1985). Moreover, there is a strong correlation between occurrence of active growth at the bud tip and clustering of cortical actin patches at the same tip. Cortical actin patches are concentrated at the site of bud emergence on unbudded cells and in small and medium size buds in budding cells, whereas actin fibers are generally oriented along the long axes of the mother-bud pairs (Adams and Pringle, 1984; Kilmartin and Adams, 1984). Near the end of the cell cycle, cortical actin patches concentrate in the neck region connecting the mother cell to its bud. However, it is not clear how the actin cytoskeleton is linked to bud assembly at the membrane.

Genetic approaches have been exploited in *S. cerevisiae* to identify genes that are required for assembly and growth of a bud. Genes *CDC24* and *CDC42* have been identified to be necessary for bud site assembly (Sloat et al., 1981; Adams et al., 1990; Johnson and Pringle, 1990). Mutations in these genes do not result in bud formation, but in an overall increase of cell surface. In these mutants, cortical actin patches uniformly distribute over the entire cell surface. The *CDC42* and *CDC24* genes encode a small guanosine 5'-triphosphate (GTP)[1]-binding protein (small G protein) (Johnson and Pringle, 1990) and a putative guanine nucleotide exchange protein for Cdc42p (Hart et al., 1991), respectively. Two other genes encoding small G proteins, *RHO3* and *RHO4*,

The present address of W. Yamochi is Department of Internal Medicine (1st Division), Kobe University School of Medicine, Kobe 650, Japan.

The present address of K. Tanaka, H. Nonaka, and Y. Takai is Department of Molecular Biology and Biochemistry, Osaka University Medical School, 2-2 Yamada-oka, Suita 565, Japan.

The present address of T. Musha is Division of Cardiovascular Pharmacology, Eisai Co., Ltd., 1-3-5 Tokaidai, Tsukuba, Ibaraki 300-26, Japan.

Address all correspondence to Y. Takai, Department of Molecular Biology and Biochemistry, Osaka University Medical School, 2-2 Yamada-oka, Suita 565, Japan.

1. *Abbreviations used in this paper*: 5-FOA, 5-fluoro-orotic acid; G protein, GTP-binding protein; GDI, GDP dissociation inhibitor; GDP, guanosine 5'-diphosphate; GDS, GDP dissociation stimulator.

Table I. Yeast Strains Used in this Study

Strain	Genotype
MM50	MATα *ura3 leu2 trp1 his3 ade2 can1 rho1::HIS3 pMM105*
RAY-3A-D-1C	MATa *ura3 leu2 trp1 his3*
RAY-3A-D	MATa/MATα *ura3/ura3 leu2/leu2 trp1/trp1 his3/his3*
KT110-1A	MATa *ura3 leu2 trp1 his3 ade2 rho1::HIS3* pMM105
TM2-1A	MATa *ura3 leu2 trp1 his3 ade2 rho1::HIS3* YCp-LEU2-GAL1-RHO1
TM2-1A-D	MATa/MATα *ura3/ura3 leu2/leu2 trp1/trp1 his3/his3 ade2/ade2 rho1::HIS3/rho1::HIS3* YCP-LEU2-GAL1-RHO1
HNY21	MATa *ura3 leu2 trp1 his3 ade2 rho1-104*
HNY30	MATa/MATα *ura3/ura3 leu2/leu2 trp1/trp1 his3/his3 ade2/ade2 rho1-104/rho1-104*

MM50 was repeatedly back-crossed to our standard wild-type strain, RAY-3A-D-1C, to construct KT110-1A. All other strains were congenic to RAY-3A-D-1C.

have recently been shown to be involved in the control of bud growth (Matsui and Toh-e, 1992).

In the mammalian system, evidence is accumulating that small G proteins regulate various cell functions (Hall, 1990; Bourne et al., 1991; Takai et al., 1992). Of the many small G proteins, the Rho family, consisting of three members, A, B, and C, has been suggested to regulate the actomyosin system. This is based on the observations that *Clostridium botulinum* ADP-ribosyltransferase, C_3, which selectively ADP-ribosylates the Rho family (Aktories et al., 1988; Kikuchi et al., 1988; Narumiya et al., 1988), changes stress fibers (Paterson et al., 1990; Ridley and Hall, 1992). Moreover, it has recently been shown that *Rho*A plays an important role in various actomyosin-dependent cell functions, including cell morphology (Rubin et al., 1988; Paterson et al., 1990; Miura et al., 1993), smooth muscle contraction (Hirata et al., 1992), platelet aggregation (Morii et al., 1992), cell motility (Takaishi et al., 1993, 1994), cytokinesis (Kishi et al., 1993), lymphocyte aggregation (Tominaga et al., 1993), lymphocyte-mediated cytotoxicity (Lang et al., 1992), and membrane ruffling (Nishiyama et al., 1994).

Rho has guanosine 5'-diphosphate (GDP)-bound inactive and GTP-bound active forms which are interconvertible by GDP/GTP exchange and GTPase reactions. The conversion from the GDP-bound inactive form to the GTP-bound active form is regulated by GDP/GTP exchange proteins and the reverse conversion is regulated by GTPase-activating proteins. There are two types of GDP/GTP exchange proteins for Rho; one is a stimulatory type, named *Smg* GDP dissociation stimulator (GDS) (Kaibuchi et al., 1991) and *Rho* GDS (Isomura et al., 1990), and the other is an inhibitory type, named *Rho* GDP dissociation inhibitor (GDI) (Fukumoto et al., 1990). We have recently demonstrated that a proto-oncogene product, Dbl, acts as a GDS for Rho (Yaku et al., 1994). Recently, a homologue closely related to *Rho* GDI has been found and shown to be expressed in hematopoietic cells (Lelias et al., 1993). Rho undergoes three kinds of post-translational modifications in the COOH-terminal region: geranylgeranylation of the cysteine residue, removal of the three COOH-terminal amino acids, and carboxyl methylation of the exposed cysteine residue (Katayama et al., 1991). *Rho* GDI and *Smg* GDS are active on only the posttranslationally processed form of RhoA (Hori et al., 1991; Mizuno et al., 1991), whereas Dbl is active on both the posttranslationally processed and unprocessed form of RhoA, but is much more active on the former than on the latter form (Yaku et al., 1994).

In the cytosol of resting smooth muscle and insulinoma cells, Rho is present in the GDP-bound inactive form complexed with *Rho* GDI (Kuroda et al., 1992; Regazzi et al., 1992), and the inhibitory action of *Rho* GDI in the GDP/GTP exchange reaction is stronger than the stimulatory action of *Smg* GDS, *Rho* GDS, or Dbl if both are present (Kikuchi et al., 1992; Kuroda et al., 1992; Yaku et al., 1994). On the basis of these observations, we have tentatively proposed the following modes of activation and action of Rho. In resting cells, the posttranslationally processed form of Rho is present in the cytosol as the GDP-bound inactive form complexed with *Rho* GDI. Upon stimulation with some signals, the inhibitory action of *Rho* GDI is released in an unknown manner, the GDP-bound inactive form of Rho becomes sensitive to the action of *Smg* GDS, *Rho* GDS, or Dbl, and the GTP-bound active form is produced. By this activation, Rho interacts with its effector protein and exerts its biological function through this effector protein.

A homologue of mammalian *Rho*A gene, *RHO1*, has been identified in *S. cerevisiae* (Madaule et al., 1987). The amino acid sequence of Rholp is ~70% identical with that of RhoA, and Rholp like RhoA has been shown to be ADP-ribosylated by C_3 (McCaffrey et al., 1991). A gene disruption experiment on *RHO1* indicates that *RHO1* is an essential gene, but the cellular function of *RHO1* remains to be clarified. In this report, we have isolated a temperature-sensitive mutation of the *RHO1* gene. The *rho1* mutation results in accumulation of tiny- or small-budded cells at nonpermissive temperature. Consistently, immunofluorescence study demonstrates that Rholp is localized at the periphery of the bud emergence sites or of the tips of growing buds. Cortical actin patches are overlappingly clustered to the Rholp-staining sites. We describe the function of *RHO1* in the process of bud formation.

Materials and Methods

Strains, Media, and Cell Growth Conditions

Yeast strains used in this study are listed in Table I. *Escherichia coli* DH5α was used for the construction and propagation of plasmids. Yeast strains were grown on a rich medium, YPD, which contained 1% Bacto-yeast extract (Difco Laboratories, Detroit, MI), 2% Bacto-peptone (Difco), 2% glucose, 0.04% adenine, and 0.02% uracil. Yeast transformations were performed by lithium acetate methods (Ito et al., 1983; Gietz et al., 1992), and other standard yeast genetic manipulations were performed as described by Sherman et al. (1986). Transformants were grown in SD medium which contained 2% glucose and 0.7% yeast nitrogen base without amino

acids (Difco). SG medium contained 3% galactose, 0.2% sucrose, and 0.7% yeast nitrogen base without amino acids. SD or SG medium was supplemented with amino acids or bases when required. SD lacking uracil (SD-ura), SG lacking uracil, SD lacking leucine, and SG lacking leucine were used for the selection of transformants. SD+5-fluoro-orotic acid (5-FOA) (Sigma Chemical Co., St. Louis, MO) medium was prepared as described previously (Boeke et al., 1984). Viable cell count was determined by plating appropriately diluted culture of the *rho1-104* mutant incubated at 24 or 37°C. Cell lysis was examined by assaying alkaline phosphatase activity using a chromogenic substrate 5-bromo-4-chloro-3-indolyl-phosphate (BCIP) (Sigma Chemical Co.) as described previously (Paravicini et al., 1992). Flow cytometric analysis was performed as described previously (Ninomiya-Tsuji et al., 1991).

Plasmid Constructions

Standard molecular biological techniques were performed to construct plasmids (Sambrook et al., 1989). The plasmid pWT consists of the wild-type 1.4-kbp *Eco*RI–*Eco*RI restriction fragment containing *RHO1* cloned into the *URA3*-bearing high copy number vector YEp352 (Madaule et al., 1987). The 2.2-kbp *Sau*I–*Bgl*II genomic fragment contained ~1.2 kbp upstream and 414 bp downstream noncoding regions. This fragment was cloned into the *URA3*-bearing single copy vector pRS316 (Sikorski and Hieter, 1989) to construct a plasmid pRS316-RHO1. A 6-bp nontranslated sequence in pRS316-RHO1, AGAAAG, which is located immediately upstream of the *RHO1* open reading frame, was changed to the *Kpn*I site, GGTACC, by use of the in vitro mutagenesis technique to construct a plasmid pRS316-RHO1 (KpnI) (Higuchi, 1989). Synthetic oligonucleotides encoding the HA epitope, YPYDVPDYA, which is derived from the influenza hemagglutinin protein, was cloned into the *Kpn*I site of pRS316-RHO1 (KpnI) to construct pRS316-HA-RHO1, which has two copies of the HA epitope (Wilson et al., 1984; Field et al., 1988; Kolodziej and Young, 1991). The 2.2-kbp DNA fragment of the *HA-RHO1* gene was cloned into the *URA3*-bearing multicopy vector, YEp352 (Hill et al., 1986), and integration vector, pRS306 (Sikorski and Hieter, 1989), to construct YEp352-HA-RHO1 and pRS306-HA-RHO1, respectively. A plasmid pRS316-HA-rhol (C206S) was constructed from pRS316-HA-RHO1 by changing G617 to C in the *RHO1* open reading frame by use of the in vitro mutagenesis technique, which caused an amino acid substitution of cysteine 206 of Rholp to serine. Expected changes of DNA sequence induced by in vitro mutagenesis or by the insertion of oligonucleotides were confirmed by DNA sequencing. The *Eco*RI-*Sal*I PCR fragments containing the *RHO1* and *Rho*A open reading frames were cloned into YCp-LEU2-GAL1, which carried the *LEU2* marker and the *GAL1* promoter on a single copy plasmid, to construct YCp-LEU2-GAL1-RHO1 and YCp-LEU2-GAL1-RhoA, respectively.

Hydroxylamine Mutagenesis

The plasmid pWT was mutagenized in vitro by hydroxylamine as described (Rose and Fink, 1987). Briefly, 10 μg of pWT DNA was added to 500 μl of a fresh hydroxylamine solution (0.09 g NaOH and 0.35 g hydroxylamine–HCl in 5 ml ice-cold water), and the reaction mixture was incubated at 37°C for 20 h. Plasmid DNA was recovered by precipitation at −80°C in ethanol, and was transformed into a yeast strain TM2-1A. The *rho1::HIS3* disruption mutation in TM2-1A was previously made by replacing the 460-bp *Eco*RI-*Cla*I fragment of *RHO1* with the *HIS3* DNA fragment (Madaule et al., 1987).

Construction of the rho1-104 Mutant

The genomic *rho1::HIS3* disrupted gene was replaced with the *rho1-104* gene by pop-in/pop-out replacement (Rothstein, 1991). The *Kpn*I-*Sac*I DNA fragment containing the *rho1*-104 mutant gene was cut out from pRS316-rhol-104 and was cloned into the *Kpn*I-*Sac*I site of an integration vector pRS306 (Sikorski and Hieter, 1989). The resulting plasmid pRS306-rhol-104 was cut at the *Hpa*I site located 22 bp downstream of the *RHO1* open reading frame and was subsequently transformed into TM2-1A. A transformant of TM2-1A in which pRS306-rhol-104 was targeted at the *RHO1* locus was selected by Southern hybridization analysis. Since the recombination occurred downstream of the *HIS3* insertion site, a second recombination upstream of *HIS3* would give rise to a strain in which the *rho1::HIS3* gene is replaced by the *rho1*-104 gene. The resulting strain would show a Ura$^-$, His$^-$, and temperature-sensitive growth phenotype. Cells of the transformant were spread on a plate containing 5-FOA to select Ura$^-$ clones as described (Boeke et al., 1984). Among 5-FOA-resistant clones His$^-$ clones were searched for and one of such clones, HNY21, was isolated. Southern hybridization analysis confirmed that the *rho1::HIS3* gene was replaced by the *rho1*-104 gene in HNY21. The temperature-sensitive growth phenotype of HNY21 was suppressed by pRS316-RHO1.

Western Blot Analysis of Rholp

HA-Rhol proteins expressed in yeast cells were detected by Western blot analysis with 12CA5 mAb (Wilson et al., 1984; Field et al., 1988). Total yeast protein was extracted from exponentially growing cells by the method described previously (Kuchler et al., 1993). About 1×10^8 cells grown in YPD medium were harvested by brief centrifugation, washed once in a lysis buffer (10 mM Tris–HCl and 1 mM EDTA, pH 7.5, containing 2% 2-mercaptoethanol and 100 μM *p*-amidinophenyl methanesulfonyl fluoride–HCl), and resuspended in 500 μl of the same cold lysis buffer. All subsequent steps were carried out at 4°C. About 1 g of prechilled glass beads (0.45-mm diam) were added to the cell suspension and lysis was achieved by vigorous vortex mixing for five 2-min intervals with 1 min of cooling in between. The resulting homogenates were collected and unbroken cells, glass beads, and large debris were removed twice by centrifugation for 5 min at 450 *g*. Membranes were collected from the clarified lysate by sedimentation for 1 h at 100,000 *g*. The particulate fraction was rinsed with the lysis buffer and resuspended in the same buffer. 60 μg of each protein sample from the homogenates and the cytosolic and particulate fractions was subjected to SDS-PAGE and separated proteins were electrophoretically transferred to a nitrocellulose membrane sheet (BA85, pore size: 0.45 μm; Schleicher & Schuell Inc., Keene, NH). The sheet was processed to detect HA-Rholp with 10 μg/ml of affinity-purified 12CA5 mAb as a primary antibody by using the ECL detection kit (Amersham Corp., Arlington Heights, IL).

Cytological Techniques

For staining of actin and DNA in *rho1* mutants, cells cultured under the permissive or restrictive conditions were fixed with 4% of formaldehyde at 25°C for 30 min. After washing once with PBS, cells were stained with rhodamine phalloidin (Molecular Probes, Inc., Eugene, OR) at a final concentration of 0.5 μM for 30 min (Adams and Pringle, 1991). After washing three times with PBS, cells were costained with 4',6'-diamidino-2-phenylindole dihydrochloride (DAPI) (Sigma Chemical Co.) at a final concentration of 0.1 μg/ml for 15 min. After washing twice with PBS, cells were observed and photographed on Neopan Super Presto film (Fuji Photo Film, Tokyo, Japan) using a Zeiss Axiophot microscope (Carl Zeiss, Oberkochen, Germany).

To visualize the intracellular localization of HA-Rholp, yeast cells expressing HA-Rholp were processed for immunofluorescence microscopy by the methods of Pringle et al. (1991). Cells were fixed with 4% of formaldehyde at 25°C for 2.5 h. Affinity-purified 12CA5 mAb was used as a primary antibody at a concentration of 25 μg/ml and the FITC-conjugated goat anti-mouse IgG (Cappel Laboratories, Malvern, PA) was used as a secondary antibody at a concentration of 10 μg/ml. After washing with PBS, cells were costained with rhodamine phalloidin. Stained cells were observed and photographed as described above.

Results

Isolation of a Temperature-sensitive Mutation in RHO1

The *RHO1* gene has been demonstrated to be essential for vegetative growth of cells in *S. cerevisiae* (Madaule et al., 1987). To explore the function of the *RHO1* gene, a conditional mutation of *RHO1*, which is a temperature-sensitive mutation, was isolated. An episomal plasmid bearing the *RHO1* and *URA3* genes, pWT-RHO1, was mutagenized with hydroxylamine as described in Materials and Methods. This mutagenized plasmid DNA was directly transformed into the yeast strain TM2-1A, which carried the *rho1* mutation disrupted with *HIS3* and a plasmid, YCp-LEU2-GAL1-RHO1, bearing the *GAL1-RHO1* gene and the *LEU2* gene. TM2-1A grows on a galactose-containing medium but not on a glucose-containing medium since the *GAL1* promoter is repressed by a glucose. Transformants were selected on SD-

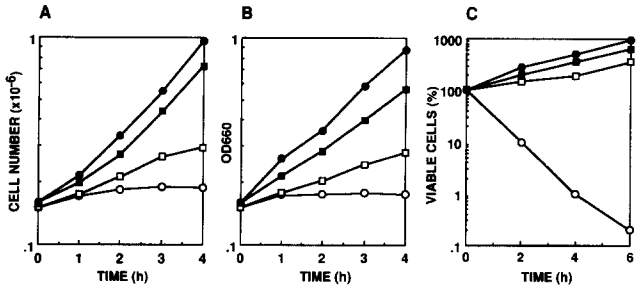

Figure 1. Cell growth and cell viability curves of the *rhol-104* mutant cells. Cells growing exponentially at 24°C of the wild-type strain RAY-3A-D (■, ●) or the *rhol-104* mutant strain HNY30 (*rhol-104/rhol-104*) (□, ○) were incubated at 24°C (■, □) or at 37°C (●, ○) for the indicated times. Timecourses of cell number (more than 1,000 cells were counted for each determination) (*A*), optical density at 660 nm (*B*), or percentage of viable cells (*C*) was determined.

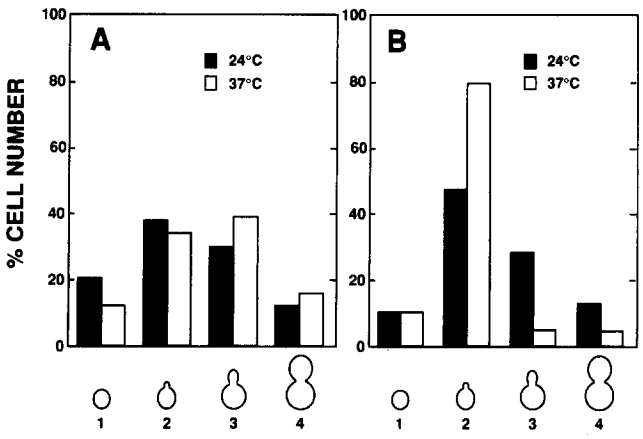

Figure 2. The terminal arrest phenotype of the *rhol-104* cells. Cells of the wild-type strain RAY-3A-D (*A*) or HNY30 (*rhol-104/rhol-104*) (*B*) were grown exponentially at 24°C and the cultures were divided into two. One was incubated at 24°C for 3 h, while the other was incubated at 37°C for 3 h. More than 1,000 cells for each strain were observed by a light microscope and the morphology of each cell was determined. (*1*) unbudded cell, (*2*) tiny- or small-budded cell, (*3*) medium-budded cell, (*4*) large-budded cell. Large-budded cell had a bud larger than about two-thirds of its mother cell in volume.

ura plate media at 24°C, and colonies were replica-plated onto SD-ura plate media which were subsequently incubated at 37°C for 2 d. From ~10,000 clones screened, candidate clones which showed temperature-sensitive growth phenotype were isolated, and the plasmids were recovered through *E. coli* transformation. One plasmid which conferred a temperature-sensitive growth phenotype on TM2-1A was identified and used for further study. The 1.4-kbp *Eco*RI-*Eco*RI restriction fragment carrying the mutant *rhol* gene was cloned into a single copy vector pRS316 (Sikorski and Hieter, 1989). This plasmid again conferred a temperature-sensitive growth phenotype on TM2-1A. The plasmid carrying the temperature-sensitive mutation of *RHO1, rhol-104*, did not retard growth of wild-type cells, indicating that the mutation was recessive.

The mutation site in *rhol-104* responsible for the temperature-sensitive trait was mapped to a 476-bp *Nhe*I-*Hpa*I restriction fragment in the *RHO1* open reading frame. DNA sequencing of this fragment of the mutant gene resulted in the identification of two transition mutations: both G214 and G491 in the *RHO1* open reading frame were changed to A. These mutations were consistent with the specificity of base changes which could be induced by the hydroxylamine mutagenesis as described (Sikorski and Boeke, 1991). The first mutation changed Asp 72 to Asn (D72N) and the second mutation changed Cys 164 to Tyr (C164Y). The D72N substitution occurred five amino acids downstream of one of the two conserved phosphate/Mg^{2+}-binding loops, Asp-Thr-Ala-Gly-Gln, while the C164Y substitution occurred at X in Glu-X-Ser-Ala, which is one of the guanine base-binding loops (Valencia et al., 1991). We have not determined which substitution is responsible for the temperature-sensitive trait of the *rhol-104* mutation.

The genomic *rhol* gene was replaced with the *rhol-104* mutant gene by the pop-in/pop-out method as described in Materials and Methods. This strain, HNY21, showed a temperature-sensitive growth phenotype which could be suppressed by a plasmid bearing the wild-type *RHO1* gene. HNY21 or its derivatives were used for further experiments.

Characterization of the rhol-104 Mutant

Examination of time courses of cell growth of the wild type and the *rhol-104* mutant cells (HNY30) indicated that the growth of the *rhol-104* cells was retarded even at 24°C and was inhibited at 37°C (Fig. 1, *A* and *B*). Neither the cell number nor optical density of the culture significantly increased at 37°C in the *rhol-104* mutant culture, suggesting that the *rhol-104* cells had halted cell growth as well as cell division. To examine whether the arrested cells lose viability or not, viable cells were counted after temperature up-shift. As shown in Fig. 1 *C*, the *rhol-104* mutant cells lost viability rapidly when incubated at 37°C, suggesting that the deficiency of cell surface growth of the arrested *rhol-104* cells were mainly due to their loss of viability. Microscopic examination of the *rhol-104* cells growing at 24°C revealed that cells with a tiny or small bud accumulated compared with the wild-type cells: 48% of the *rhol-104* cells versus 38% of the wild-type cells (Fig. 2). In contrast, in the *rhol-104* cells arrested at 37°C, the population of tiny- or small-budded cells increased up to 80%, which presented a clear contrast to 34% in the wild-type control culture (Fig. 2). To confirm that cell surface growth was inhibited at 37°C, length of the long axes of tiny- or small-budded cells was measured in more than 500 cells of the *rhol-104* mutant and wild-type cells. The average cell length of the *rhol-104* cells grown at 24°C was not longer than that of the wild-type cells grown at 24°C and did not change after incubation at 37°C for 6 h (data not shown).

Cells of the *rhol-104* mutant and the *RHO1*-depleted mutant grown under the permissive conditions or arrested under nonpermissive conditions were stained with rhodamine phalloidin and DAPI to visualize actin and DNA, respectively, by fluorescence microscopy (Fig. 3). In both mutant cells arrested as tiny- or small-budded cells, cortical actin patches were concentrated to budding sites or in buds (Fig. 3, *A* and *B*, *Actin*) as described in tiny- or small-budded cells of the wild-type strain (Adams and Pringle, 1984; Kilmartin and Adams, 1984). Tiny-budded cells were more frequently

seen in the *rhol-104* cells (~70% of tiny-budded cells and 30% of small-budded cells) than in the *RHO1*-depleted cells (~30% of tiny-budded cells and 70% of small-budded cells) (data not shown). Staining with DAPI showed that the *rhol-104* cells arrested at 37°C had a single nucleus (Fig. 3, *A* and *B, DNA*). To examine the state of nuclear DNA further, flow cytometric analysis was conducted to determine the DNA content of the arrested cells of the *rhol-104* mutant (Fig. 4). Cells of the wild-type strain RAY-3A-D or *rhol-104* mutant strain HNY30 (*rhol-104/rhol-104*) growing exponentially at 24°C were further incubated at 24, 33, or 37°C for 5 h. 65, 45, and 40% of the wild-type cells showed 4-n peaks when incubated at 24, 33, and 37°C, respectively (Fig. 4 *A*). In contrast, 70, 95, and 65% of the *rhol-104* mutant cells showed 4-n peaks when incubated at 24, 33, and 37°C, respectively. These results indicate that the nuclear cycle of the *rhol-104* cells was not arrested in a cell cycle-specific manner at 37°C, but was arrested at the G2/M phase at 33°C.

Cell cycle arrest at the small-budded stage has been observed with a mutant in *PKC1* which is a yeast homologue of mammalian protein kinase C of an $\alpha\beta\gamma$ type (Levin and Bartlett-Heubusch, 1992). Since cell lysis phenotype has also been found in the *pkc1* mutant, cell lysis of the *rhol-104* or *RHO1*-depleted cells was examined by assaying alkaline phosphatase activity which was normally localized to vacuoles (Fig. 5). This method was used to detect the cell lysis phenotype of the *pkc1* mutant (Paravicini et al., 1992). Substantial activity of alkaline phosphatase was detected in the *RHO1*-depleted cells incubated in YPD medium for 16 h (Fig. 5 *B*) and in the *rhol-104* cells incubated at 37°C for 1 h (Fig. 5, *C* and *D*). Although cell lysis was not microscopically evident in the *rhol* mutant cultures, the temperature-sensitive *pkc1* mutant was also found to release intracellular materials without apparent cell lysis at the restrictive temperature (Levin and Bartlett-Heubusch, 1992). The lethality caused by the cell lysis phenotype of the *pkc1* mutant has been found to be suppressed by an osmotic stabilizer such as 1 M sorbitol (Levin and Bartlett-Heubusch, 1992). In contrast, the lethality of the *rhol* disruption mutant was not suppressed by the presence of 1 M sorbitol in the medium, although the *rhol-104* temperature-sensitive mutant cells grew at 37°C in the presence of 1 M sorbitol (Fig. 6).

Suppression of the Growth Deficiency of the rhol Mutant by Expression of Mammalian RhoA

Among the mammalian small G proteins, the mammalian RhoA protein is the most similar to the yeast Rholp (Madaule et al., 1987). We examined whether expression of the *Rho*A gene could replace the function of the *RHO1* gene. For this purpose, human *Rho*A cDNA was cloned into a yeast single copy expression vector, YCp-LEU2-GAL1. The resulting plasmid, YCp-LEU2-GAL1-RhoA, expressed *Rho*A under control of the *GAL1* promoter. A strain KT110-1A carried the *rhol* gene disrupted with *HIS3* and the resulting lethality was suppressed by the presence of the plasmid pMM105, a *URA3*-bearing single copy plasmid containing the *GAL10-RHO1* gene. KT110-1A was transformed with YCp-LEU2-GAL1-RHO1, YCp-LEU2-GAL1-RhoA, or a vector plasmid, YCp-LEU2-GAL1. Transformants which grew on the SG-ura-leu medium at 30°C were streaked on the SG-ura-leu medium containing uracil and 5-FOA. The plate was subsequently incubated at 24°C for 4 d. Since 5-FOA inhibits the growth of Ura$^+$ cells, only cells that had lost pMM105 should grow on the 5-FOA–containing medium. As shown in Fig. 7, cell growth on the 5-FOA–containing medium was seen with cells bearing YCp-LEU2-GAL1-RhoA as well as YCp-LEU2-GAL1-RHO1. Therefore, expression of *Rho*A suppressed the growth deficiency of the *rhol* disruption mutant, although the suppression was not seen when incubated at 37°C (data not shown). Suppression of growth deficiency of the *rhol* disruption mutant was also seen with a single copy plasmid carrying the *Rho*A gene under the control of the *RHO1* promoter (data not shown). These results suggest that mammalian RhoA is functionally homologous to yeast Rhol protein, in addition to the structural homology.

Intracellular Localization of Rholp

Phenotypic analysis of the *rhol-104* temperature-sensitive mutant and the *RHO1*-depleted mutants suggested that *RHO1* is involved in the process of bud growth. Indirect immunofluorescence method was used to reveal the intracellular localization of Rholp. For this purpose, oligonucleotides encoding the HA epitope of influenza hemagglutinin were added to the 5′ end of the *RHO1* open reading frame. The promoter region of the *RHO1* gene of this construct was kept intact not to alter the expression level of the *RHO1* gene. This *RHO1* gene tagged with the HA epitope was cloned into a single copy vector, pRS316, and an integration vector, pRS306, to construct plasmids pRS316-HA-RHO1 and pRS306-HA-RHO1, respectively. Plasmid pRS316-HA-RHO1 suppressed the temperature-sensitive growth phenotype of HNY30 (*rhol-104/rhol-104*) as well as the lethality of TM2-1A-D (*rhol::HIS3/rhol::HIS3*). The lethality of TM2-1A-D was also suppressed by integrating pRS306-HA-RHO1 at the *rhol::HIS3* locus. These *rhol* mutant cells expressing *HA-RHO1* were morphologically indistinguishable from the wild-type cells. These results indicate that HA-Rholp functions as wild-type Rholp.

Cells of three strains described above carrying the *HA-RHO1* gene were grown at 30°C and processed for indirect immunofluorescence microscopic analysis. To visualize the HA-Rhol protein, cells were stained with 12CA5 mAb and subsequently with the FITC-conjugated goat anti-mouse IgG antibody. The same preparation was doubly stained with rhodamine phalloidin to visualize actin. The results are shown in Fig. 8. Distribution of cortical actin patches at specific stages of cell cycle is well established in *S. cerevisiae* (Adams and Pringle, 1984; Kilmartin and Adams, 1984). In the small unbudded cells, cortical actin patches distributed randomly on the cell surface (Fig. 8, *A*, *B*, and *C*, *1*, *Actin*) and the staining with 12CA5 mAb was seen in the cytoplasm (Fig. 8, *A*, *B*, and *C*, *1*, *HA-Rholp*). This is consistent with the result that the substantial portion of HA-Rholp was present in the cytosolic fraction as estimated by Western blot analysis (see below). However, at least a part of the staining with 12CA5 was due to nonspecific staining, since 12CA5 mAb similarly stained the cytoplasm of cells which did not express the HA epitope (Fig. 8, *A*, *B*, and *C*, *1*, *Control*). In the large unbudded cells, cortical actin patches were concentrated at the site where budding would occur (Fig. 8, *A*, *B*, and *C*, *2*, *Actin*). In these cells, HA-Rholp was found to be colocalized with cortical actin patches, although HA-Rholp was stained uniformly at the periphery of cells (Fig.

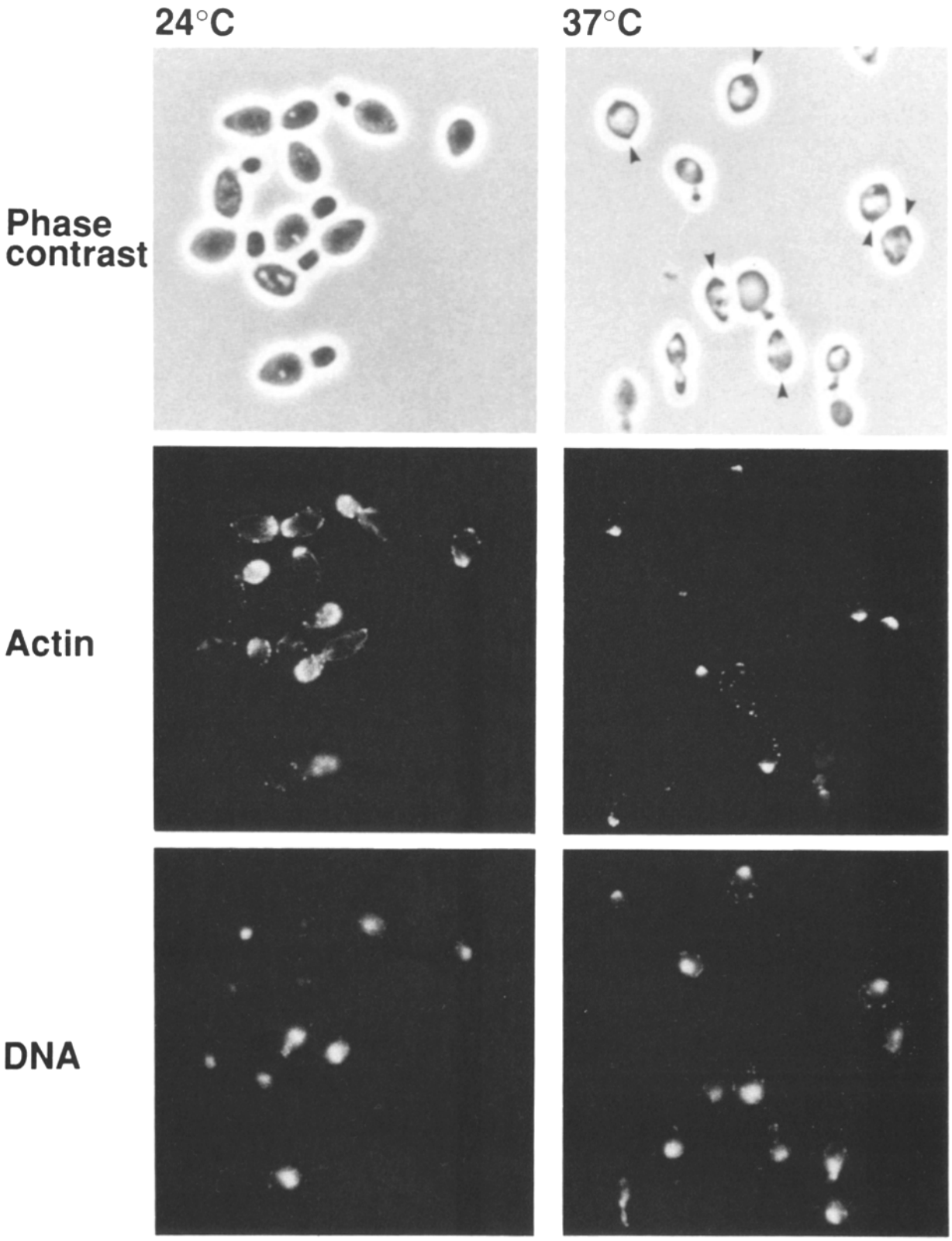

Figure 3. Morphology of the *rhol-104* (*A*) and the *RHO1*-depleted cells (*B*). Asynchronous culture of a diploid strain HNY30 (*rhol-104/rhol-104*) grown at 24°C was further incubated at 24°C or at 37°C for 3 h. Asynchronous culture of a diploid strain TM2-1A-D (*rhol::HIS3/rhol::HIS3*) grown at 30°C in YPGal medium was further incubated in YPGal or in YPD medium for 15 h. Fixed cells were then stained with rhodamine phalloidin (*Actin*) and with DAPI (*DNA*), and the stained cells were observed under a light (*Phase contrast*) or fluorescence microscope. Tiny buds of the *rhol-104* cells arrested at 37°C are shown with arrowheads.

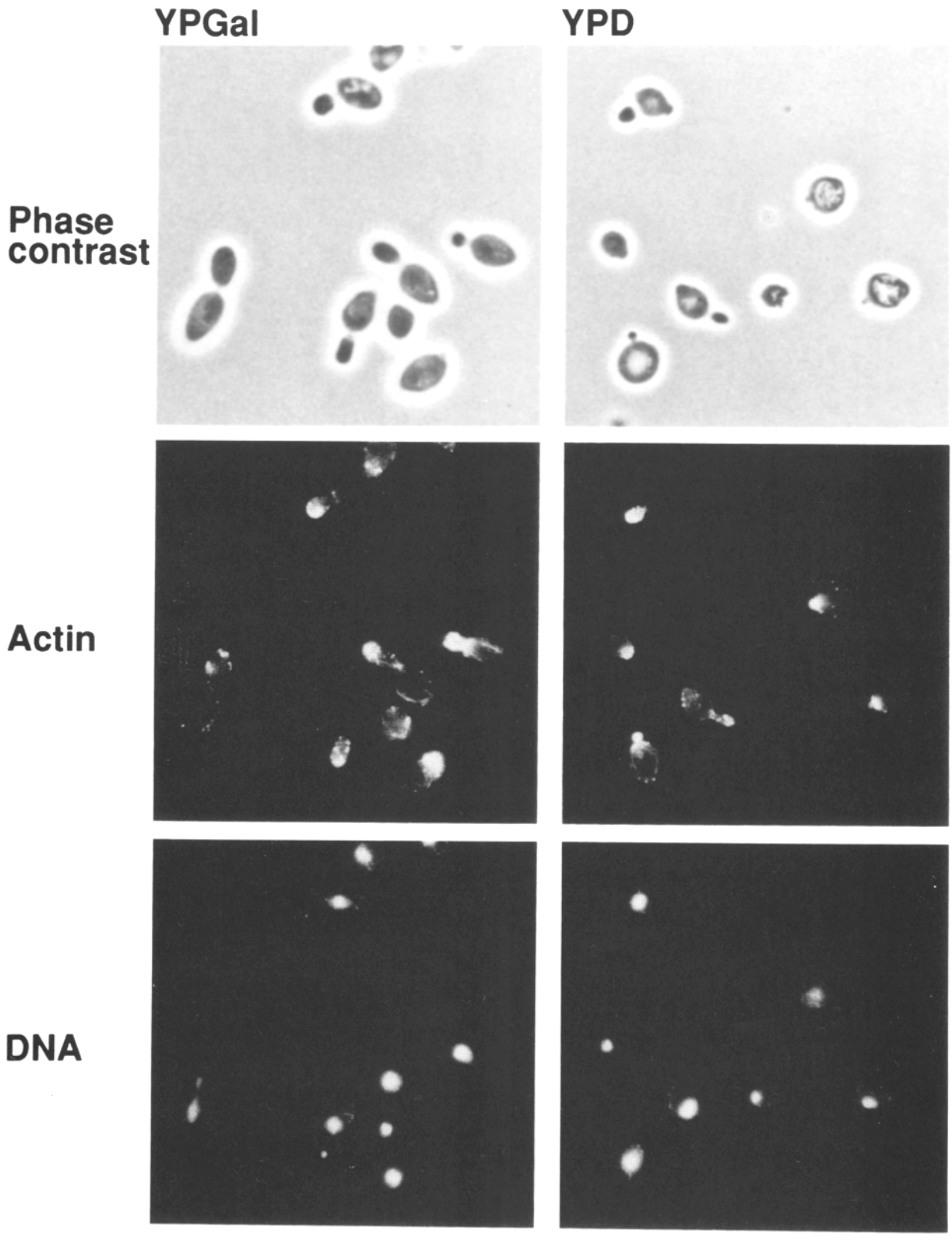
B
YPGal
YPD
Phase contrast
Actin
DNA

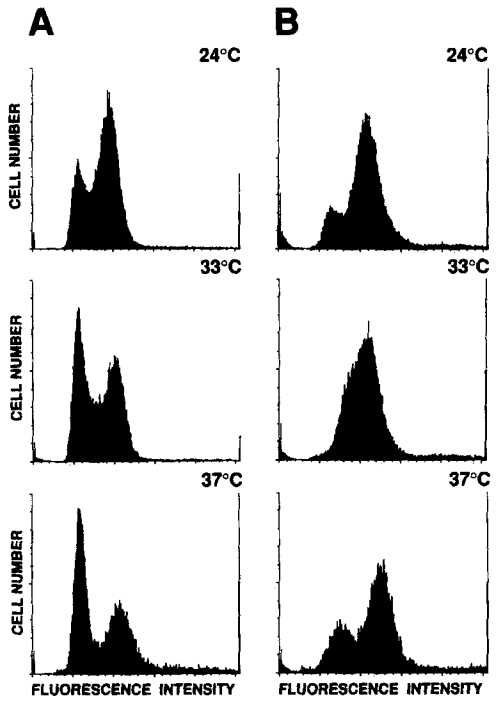

Figure 4. Flow cytometric analysis of the *rho1* mutant. Cells of the wild-type strain RAY-3A-D (*A*) or *rho1-104* mutant strain HNY30 (*B*) growing at 24°C were further incubated at 24, 33, or 37°C for 5 h. Flow cytometric analysis of DNA contents was subsequently conducted on these cells.

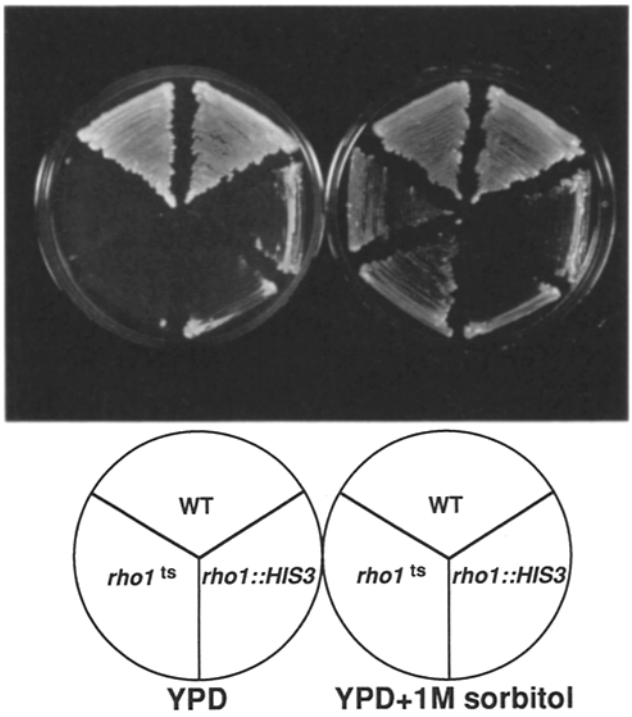

Figure 6. Suppression of the temperature-sensitive growth phenotype of the *rho1-104* cells by osmotic stabilizer. The wild-type strain RAY-3A-D (*WT*), *rho1* disruption mutant TM2-1A-D (*rho1::HIS3*), and *rho1-104* temperature-sensitive mutant HNY30 (*rho1*^{ts}) were streaked on YPD and YPD+1 M sorbitol media and incubated at 37°C for 3 d. Residual growth of TM2-1A-D seems to be due to a time lag for the repression of the *GAL1* promoter.

8, *A*, *B*, and *C*, *2*, *HA-Rho1p*). In cells forming small buds, cortical actin patches were localized into the buds as well as to the budding sites (Fig. 8, *A*, *B*, and *C*, *3*, *Actin*). In these cells, HA-Rho1p was localized to the periphery covering the entire buds (Fig. 8, *A*, *B*, and *C*, *3*, *HA-Rho1p*). In cells with larger buds in which cortical actin patches were concentrated towards the bud tips (Fig. 8, *A*, *B*, and *C*, *4*, *Actin*), staining of Ha-Rho1p was also dense around the bud tips (Fig. 8, *A*, *B*, and *C*, *4*, *HA-Rho1p*). It is known that cortical actin patches randomly redistribute throughout mother and daughter cells after the G2 phase, but before cytokinesis (Adams and Pringle, 1984; Kilmartin and Adams, 1984) (Fig. 8, *A*, *B*, and *C*, *5*, *Actin*). Staining of HA-Rho1p was hardly seen in these cells (Fig. 8, *A*, *B*, and *C*, *5*, *HA-Rho1p*). Following mitosis, cortical actin patches became clustered at the mother–bud neck region before cytokinesis (Fig. 8, *A*, *B*, and *C*, *6*, *Actin*). HA-Rho1p was localized again at the periphery of cells where cortical actin patches clustered in these cells (Fig. 8, *A*, *B*, and *C*, *6*, *HA-Rho1p*). The staining of HA-Rho1p at the cytokinesis site raised a possibility that unbudded cells with HA-Rho1p colocalized with cortical actin patches were in the postcytokinetic stage. To answer this question, the appearance of HA-Rho1p at the presumptive budding site was observed on cells emerging from stationary phase. Cells of HNY30 carrying pRS316-HA-RHO1 were grown to stationary phase in YPD medium and released into fresh YPD medium for 1 h. Cells with HA-Rho1p colocalized with actin patches at the presumptive budding site significantly increased after the 1-h incubation (data not shown). Therefore, it seems that HA-Rho1p colocalized with actin patches in cells at the budding stage.

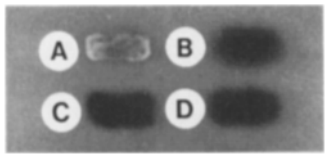

Figure 5. Cell lysis phenotype of the *rho1* mutants. Wild-type strain RAY-3A-D (*A*), *rho1* disruption mutant TM2-1A-D (*B*), and *rho1-104* temperature-sensitive mutants of a haploid strain HNY21 (*C*) and of a diploid strain HNY30 (*D*) were streaked on YPD plate, incubated at 24°C for 15 h, and then incubated further at 37°C for 1 h. The patches were stained with a chromogenic substrate, BCIP, of alkaline phosphatase for 15 h at 25°C.

Among ~500 cells observed in each HA-Rho1p–expressing strain, more than 70% of cells in large unbudded, small-budded, medium-budded, or cytokinetic cell cycle stage were stained at the growth site as shown in Fig. 8, while no such staining was observed in more than 500 observed cells of each strain carrying the *RHO1* gene in place of the *HA-RHO1* gene. Representatives of these control cells are shown (Fig. 8, *A*, *B*, and *C*, *1–6*, *Control*).

Fractionation of Rho1p into Both Cytosolic and Particulate Fractions

Results shown in Fig. 8 suggested that at least a part of HA-Rho1p might be localized to the plasma membrane. To exam-

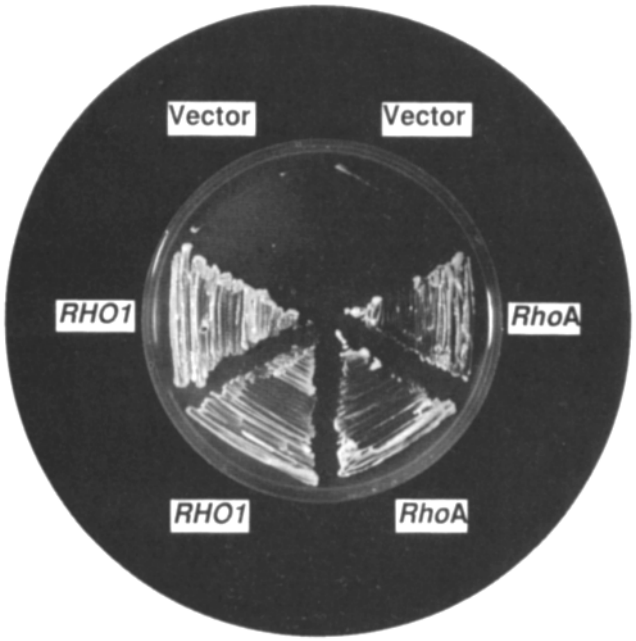

Figure 7. Suppression of the growth deficiency of the *rhol* disruption mutant by expression of the human *Rho*A gene. KT110-1A (*rhol::HIS3* pMM105), whose lethality was suppressed by the galactose-dependent expression of *RHO1* on a *URA3*-bearing single copy vector, was transformed with YCp-LEU2-GAL1-RHO1 (*RHO1*), YCp-LEU2-GAL1-RhoA (*RhoA*), or YCp-LEU2-GAL1 (*Vector*). The resulting transformants were streaked on SG-ura-leu medium containing 5-FOA and uracil. The plate after 4 d incubation at 24°C is shown.

ine this point, Western blot analysis was performed with 12CA5 mAb on the cytosolic and particulate fractions obtained by centrifugation at 100,000 *g* from cells of HNY30 bearing pRS316-HA-RHO1 or pRS316-RHO1 (Fig. 9). A protein with an M_r value of 26 kD was detected from cells expressing *HA-RHO1*, but not from cells expressing *RHO1*, indicating that the 26-kD protein was HA-Rholp (Fig. 9, *A* and *B*). About 70% of HA-Rholp was found in the cytosolic fraction (Fig. 9 *A*, lane 2), while 30% of HA-Rholp was found in the particulate fraction (Fig. 9 *A*, lane 3). HA-Rholp in the particulate and cytosolic fractions probably represented HA-Rholp stained at the sites of cell growth and cytoplasm in the immunofluorescence microscopy shown in Fig. 8, respectively. Another protein with an M_r value of 50 kD was detected from both *HA-RHO1*- and *RHO1*-expressing cells (Fig. 9, *A* and *B*). Since the 50-kD protein was detected only in the 100,000 *g* supernatant fractions, we presumed that the nonspecific staining of the cytoplasm with 12CA5 mAb in the immunofluorescence microscopy shown in Fig. 8 might be due to this 50-kD protein.

Requirement of Posttranslational Modifications for the Function and Localization of Rholp

Most small G proteins including Rholp undergo posttranslational modifications including the attachment of lipid moieties to cysteine residues at the carboxyl terminus (Katayama et al., 1991; Qadota et al., 1992). To examine whether these modifications are important for the function and localization of Rholp, the cysteine residue at amino acid position 206 was changed to serine by use of the in vitro mutagenesis technique. The *HA-rhol* (C206S) gene was cloned into a single copy plasmid pRS316 and the resulting plasmid, pRS316-HA-rhol (C206S), was transformed into the strain HNY30 (*rhol-104/rhol-104*). The transformants did not grow at 37°C, indicating that HA-rhol (C206S)p was not functional. Cells of a transformant were grown in a rich medium at 24°C and were stained with rhodamine phalloidin and with 12CA5 mAb. As shown in Fig. 10 (*rhol [C206S]p, HA*), no particular staining with 12CA5 was observed except that the cytoplasm was stained to a certain extent, suggesting that HA-rhol (C206S)p remained in the cytoplasm. Western blot analysis indicated that most of HA-rhol(C206S)p was present in the cytosolic fraction (Fig. 9 *C*, lanes 2 and 3). These results indicate that the posttranslational modifications of Rholp are essential for Rholp to localize to the site of cell growth, where, most probably, Rholp performs its function.

A Saturable Binding Site for Rholp at the Growth Site

The results described above suggest that there may be a specific binding site for Rholp at the plasma membrane in the sites of cell growth. To examine whether the binding site is saturable, we transformed HNY30 with a multicopy plasmid YEp352-HA-RHO1, which overexpressed HA-Rholp. Although very high expression of *RHO1* by a strong promoter was detrimental to the growth of cells, overexpression with the *RHO1* promoter on a multicopy plasmid affected neither the rate of cell growth nor the cell morphology (data not shown). Western blot analysis demonstrated that HA-Rholp was overexpressed about three- to fivefold both in the cytosolic and particulate fractions (Fig. 9 *D*, lanes 2 and 3). The increase of the overexpressed HA-Rholp in the cytosolic fraction might not simply be due to the incomplete posttranslational modifications of HA-Rholp, because HA-Rholp fully underwent the posttranslational modifications in the *HA-RHO1* overexpressing strain, as estimated by the SDS-PAGE method described previously (Mizuno et al., 1991), in which the posttranslationally modified RhoA migrates faster than the posttranslationally unmodified RhoA. Transformants were processed for indirect immunofluorescence microscopy with 12CA5 mAb and for staining with rhodamine phalloidin. As shown in Fig. 10 (*Rholp, overproduced*), overexpression of *HA-RHO1* did not significantly affect the distribution of cortical actin patches (*Actin*), while the staining of HA-Rholp was seen at the almost entire periphery of cells as well as in the cytoplasm irrespective of cell cycle stage (*HA*). This result suggests that the overexpressed Rholp which was recovered as the particulate fraction nonspecifically bound to the plasma membrane region. Therefore, the Rholp-binding site at the growth site seems to be saturable and there may be a specific protein which binds to Rholp at the sites of cell growth.

Discussion

Isolation of a temperature-sensitive mutation of the *RHO1* gene has revealed that *RHO1* is required for the budding process. The *rhol-104* cells were arrested in the cell cycle as tiny- or small-budded cells and no cell surface growth occurred after arrest. Since the phenotype was seen in the *RHO1*-

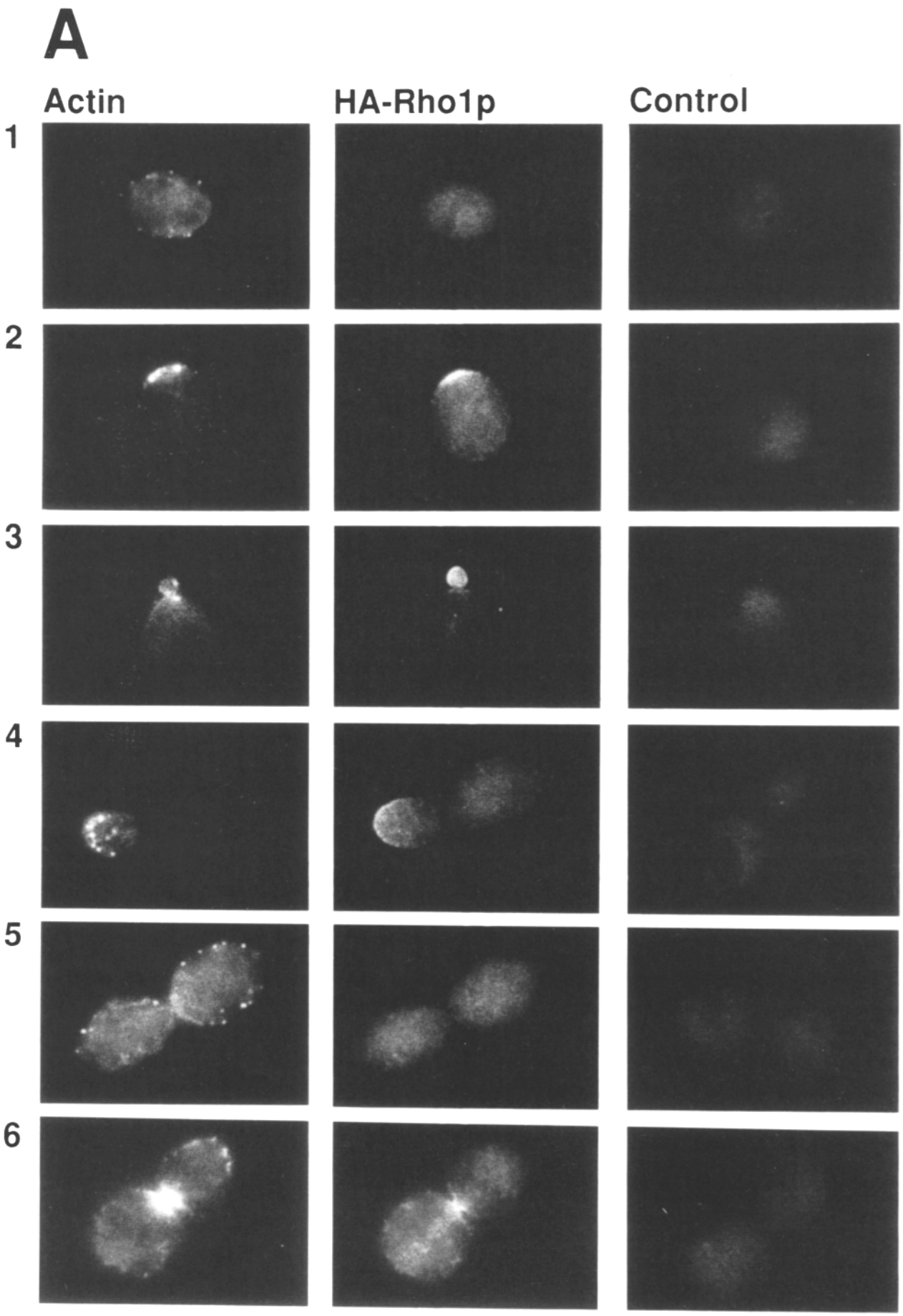

Figure 8.

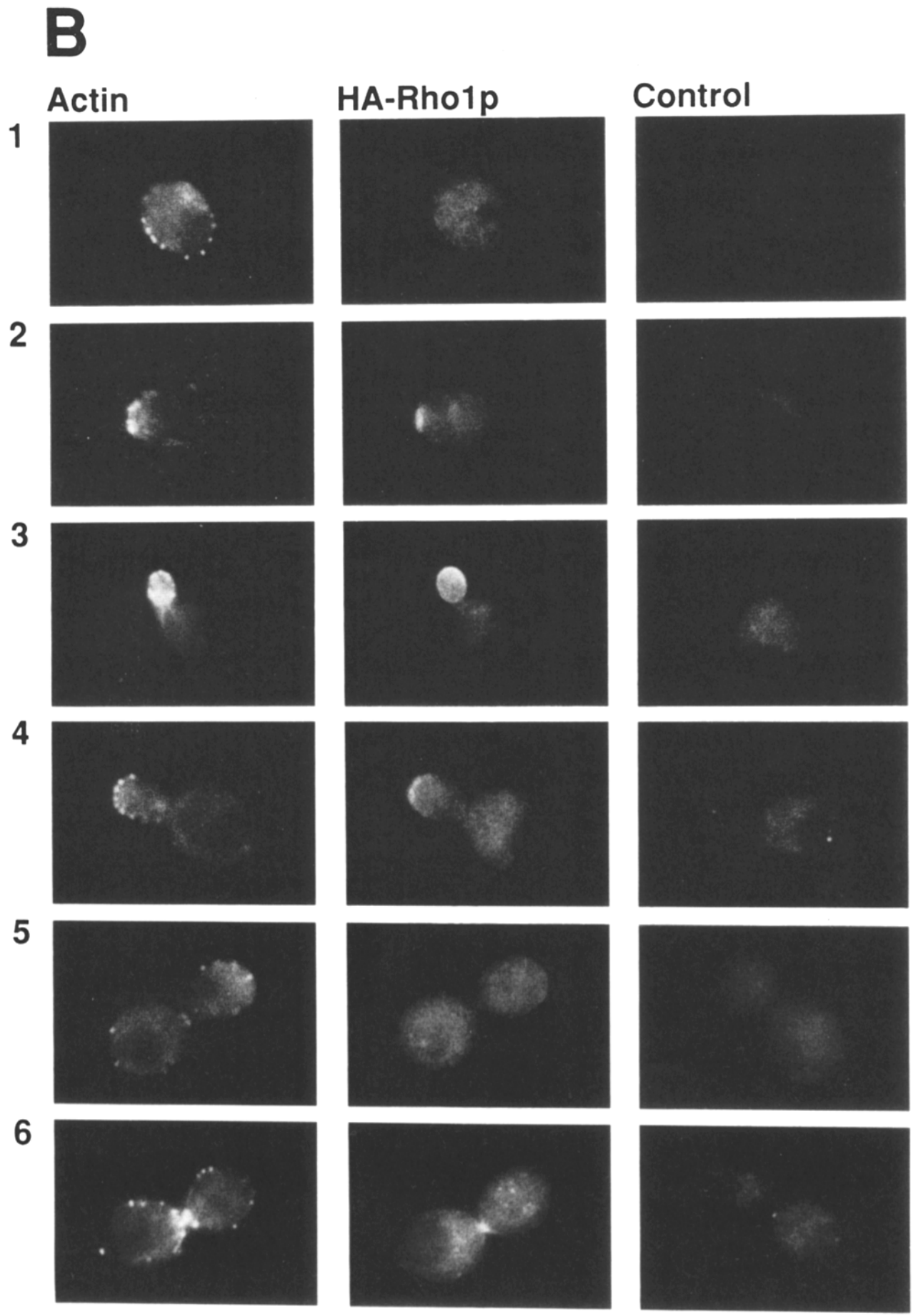

Figure 8.

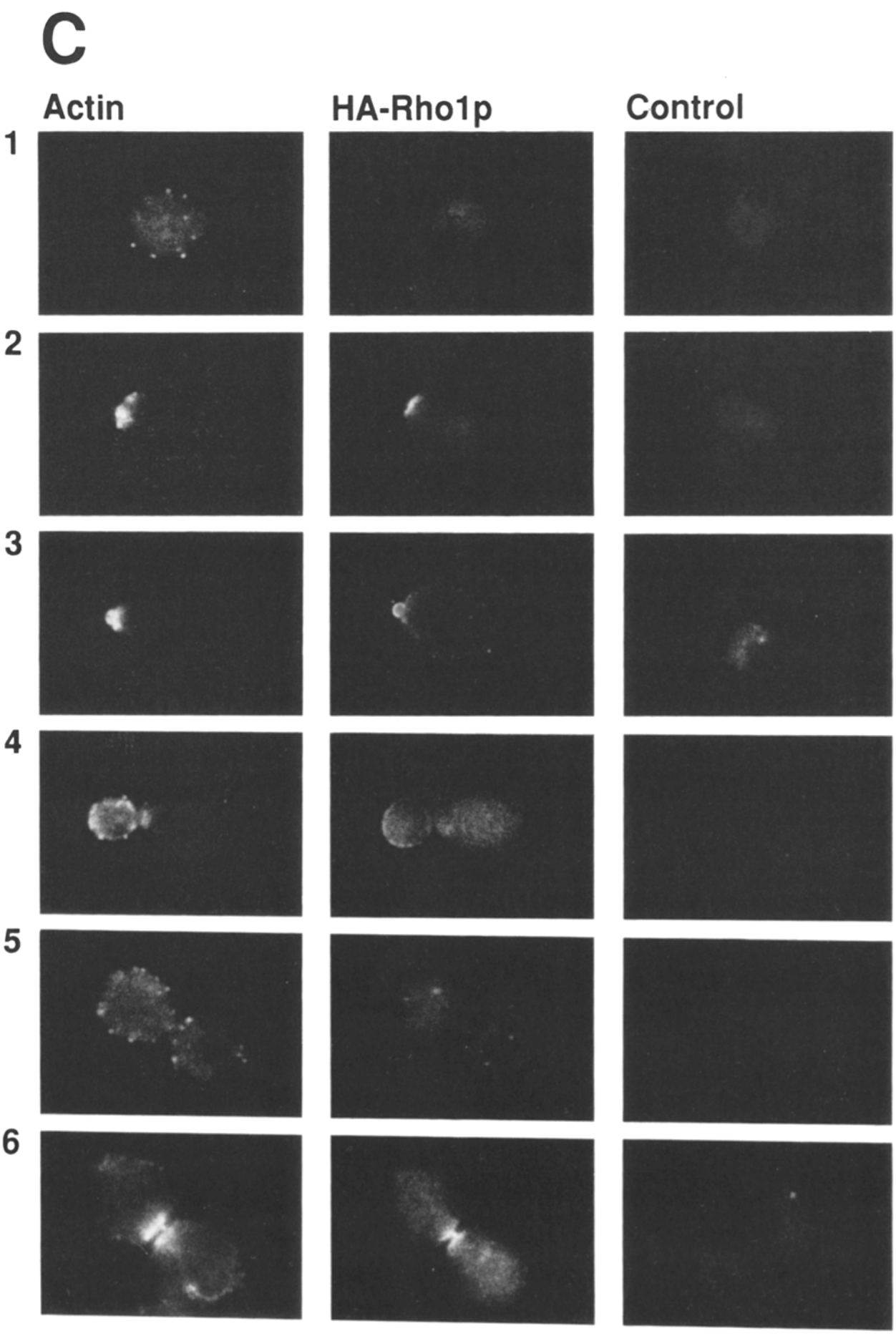
C
Actin
HA-Rho1p
Control
1
2
3
4
5
6

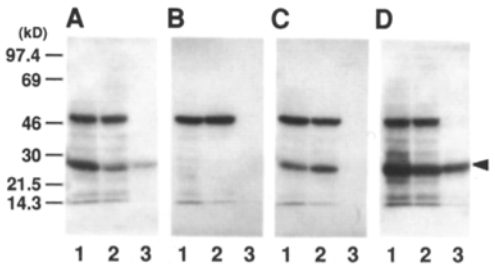

Figure 9. Western blot analysis of HA-Rholp. Cells of HNY30 expressing *HA-RHO1* on a single copy plasmid (*A*), *RHO1* on a single copy plasmid (*B*), *HA-rho1* (C206S) on a single copy plasmid (*C*), and *HA-RHO1* on a multicopy plasmid (*D*) were grown asynchronously in YPD medium at 30°C except for cells expressing *HA-rho1* (C206S), which were cultured at 24°C. Crude homogenates (lane *1*) were prepared and fractionated into cytosolic (lane *2*) and particulate fractions (lane *3*) at 100,000 *g*. Protein samples were subjected to SDS-PAGE and separated proteins were processed for Western blot analysis with 12CA5 mAb as described in Materials and Methods. The protein markers used were phosphorylase (*B*) (M_r = 97,400), bovine serum albumin (M_r = 69,000), ovalbumin (M_r = 46,000), carbonic anhydrase (M_r = 30,000), trypsin inhibitor (M_r = 21,500), and lysozyme (M_r = 14,300). An arrowhead indicates the HA-Rho1 proteins.

depleted mutant, arrest with tiny- or small-budded cells might be caused by the loss of function of Rholp. The morphological phenotype of *rho1-104* was different from those of previously described *cdc* mutants: many of the *cdc* mutants that have entered the cell division cycle continue cell growth after division has been arrested (Hartwell et al., 1974; Pringle and Hartwell, 1981). Flow cytometric analysis revealed that the nuclear cycle of the *rho1-104* mutant was not arrested in a cell cycle-specific manner at 37°C, but was arrested at the G2/M phase at 33°C. We favor a hypothesis that the *rho1-104* mutation indirectly caused the arrest of the nuclear cycle, because Rholp was localized at the sites of cell growth, not around the nuclei. Arrest of the nuclear cycle and cell growth in the *rho1-104* cells may be caused by the rapid loss of viability at the restrictive temperature.

We have noted that the phenotypes of the *rho1* mutant are similar to those of the two previously described mutants, *cdc1* and *pkc1*. The *cdc1* mutant arrests its cell division with unbudded or tiny-budded cells and loses cell viability rapidly at the restrictive temperature (Hartwell, 1971; Pringle and Hartwell, 1981). The *cdc1* mutant could complete DNA synthesis, but not nuclear division, as the *rho1-104* mutant arrested at 33°C (Hartwell, 1971; Pringle and Hartwell, 1981). Although the *RHO1* gene did not complement the *cdc1* mutation even on a multicopy plasmid (data not shown), *CDC1* might encode a protein which functions in the *RHO1*-mediated signalling pathway. The *PKC1* gene encodes a yeast homologue of mammalian protein kinase C of $\alpha\beta\gamma$ type (Levin and Bartlett-Heubusch, 1992). Cells of the galactose-dependent *pkc1* mutant arrests as small-budded cells which are not detectably enlarged. It has been also shown that temperature-sensitive *pkc1* mutant cells lose their viability at the restrictive temperature as rapidly as the *rho1-104* mutant cells did. This rapid loss of viability in the *pkc1* mutant has been shown to be caused by cell lysis which could be suppressed by osmotic stabilizer (Levin and Bartlett-Heubusch, 1992). We have noted that the *rho1-104* and *RHO1*-depleted mutants also show the cell lysis phenotype under the restrictive conditions. Recently, we have isolated a gene which suppresses the temperature-sensitive growth phenotype of the *rho1* mutant at 30°C on a multicopy vector. DNA sequencing of this gene have revealed that it is identical to *PPZ2*, encoding a type 1 protein phosphatase (T. Musha, K. Tanaka, H. Nonaka, and Y. Takai, manuscript in preparation). The *PPZ2* gene has been also isolated as a multicopy suppressor of the *pkc1* mutant (Lee et al., 1993), indicating that *RHO1* is functionally relevant to *PKC1*. One major phenotypic difference between *rho1* and *pkc1* mutants is that cell growth of a gene disruptant of *PKC1*, but not of *RHO1*, is supported by osmotic stabilizer such as 1 M sorbitol. *RHO1* plays an essential role in the bud growth and a part of the *RHO1* function may be related to the osmotic integrity which is controlled by the *PKC1* gene.

Epitope tagging method enabled us to demonstrate the intracellular localization of Rholp. Rholp was stained uniformly at the sites of cell growth where cortical actin patches clustered. Consistently, Rholp was found to be localized at the tip of shmoo-like region in the *cdc28-13* mutant cells incubated at 37°C (data not shown). In contrast, the rho1-(C206S) mutant protein seemed to remain in the cytoplasm. The rho1(C206S) protein has an amino acid substitution at the cysteine residue that receives posttranslational modifications which are important for membrane binding of GTP-binding proteins. Therefore, Rholp appears to bind to the plasma membrane or vesicles near the plasma membrane. We have recently shown that the posttranslational modifications are also required for a small G protein to activate its target protein. The posttranslational modifications are essential for Rac to activate the superoxide generation (Ando et al., 1992) and for Ras to activate adenylate cyclase in *S. cerevisiae* (Horiuchi et al., 1992) and MAP kinase in *Xenopus laevis* (Itoh et al., 1993). Therefore, there seems to be a target protein for Rholp at the sites of cell growth. It has previously been reported by immunofluorescence microscopy that Rholp is detected as a punctate pattern, with the signal concentrated toward the cell periphery and in the buds (McCaffrey et al., 1991). These stained regions have been

Figure 8. Intracellular localization of the Rho1 protein. Cells of three strains, HNY30 (*rho1-104/rho1-104*) carrying the HA-tagged *RHO1* gene on a single copy plasmid pRS316 (*A*), TM2-1A-D (*rho1::HIS3/rho1::HIS3*) carrying the same plasmid (*B*), and TM2-1A-D-T1 (*rho1::HIS3::HA-RHO1/rho1::HIS3*) in which pRS306-HA-RHO1 plasmid was integrated into one of *rho1::HIS3* loci (*C*), were grown at 30°C asynchronously in YPD medium. Cells were then fixed and processed for costaining with rhodamine phalloidin (*Actin*) and with 12CA5 mAb (*HA-Rholp*) as described in Materials and Methods. Cells of each strain carrying the *RHO1* gene in place of the *HA-RHO1* gene were also stained with 12CA5 mAb (*Control*). (*1*) Unbudded cell with uniform distribution of cortical actin patches, (*2*) unbudded cell with cortical actin patches localized at the presumptive budding site, (*3*) small-budded cell, (*4*) medium size-budded cell, (*5*) large-budded cell with uniform distribution of cortical actin patches, (*6*) large-budded cell with cortical actin patches concentrated to the mother–bud neck region.

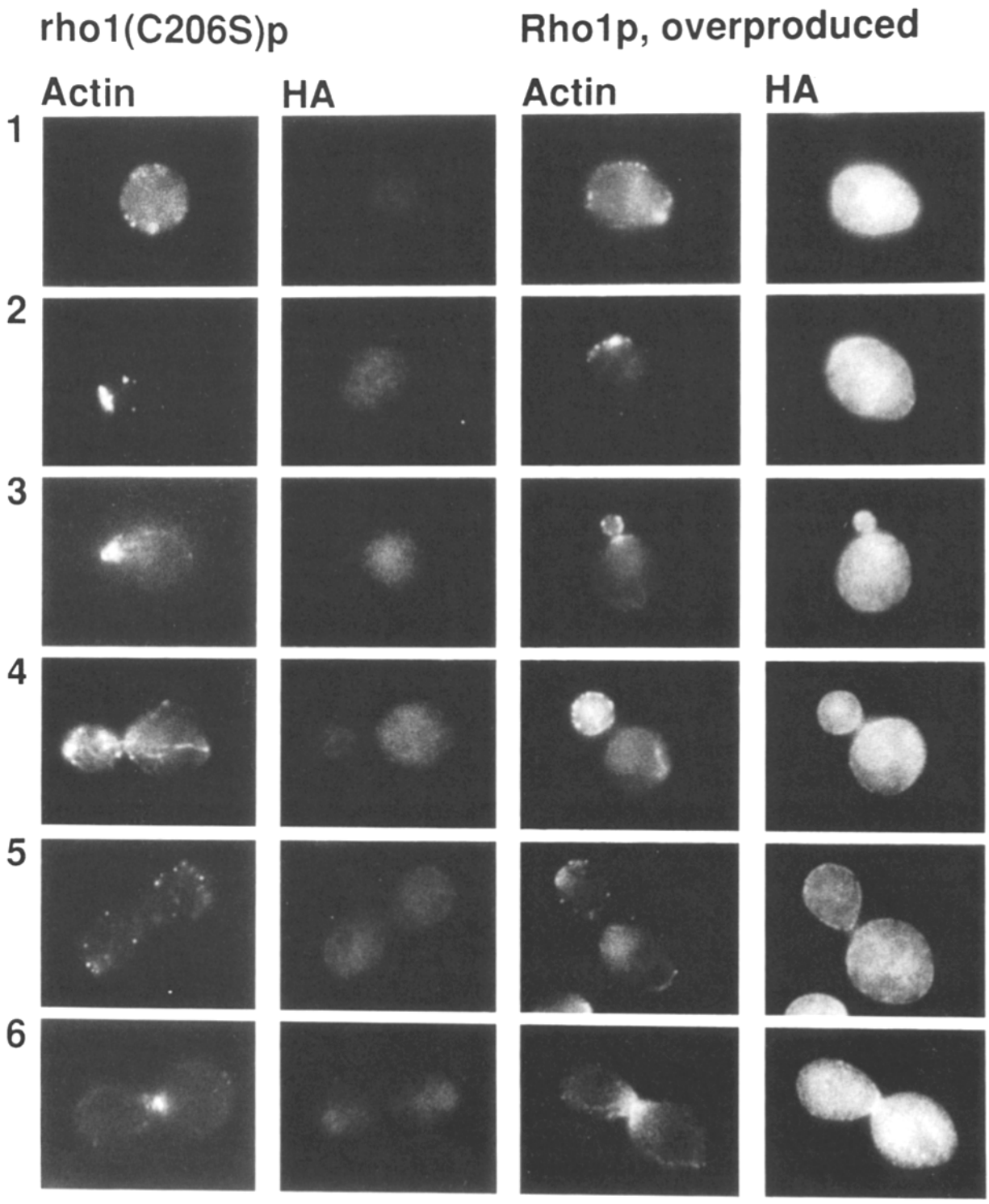

Figure 10. Intracellular localization of HA-rhol (C206S) mutant protein and overexpressed HA-Rholp. HNY30 (*rhol-104/rhol-104*) cells bearing the *HA-rhol* (C206S) gene on a single copy plasmid (*rhol(C206S)p*) or the *HA-RHO1* gene on a multicopy plasmid (*Rholp, overproduced*) were fixed and costained with rhodamine phalloidin (*Actin*) and with 12CA5 mAb (*HA*) as described in Materials and Methods. Cells at various cell cycle stages (*1–6*) as in Fig. 8 are shown.

proposed to be post-Golgi vesicles by subcellular fractionation experiments (McCaffrey et al., 1991). HA-Rholp was also stained at the peripheral regions of buds in our immunofluorescence microscopic study. However, we did not see any vesicle-like staining pattern of HA-Rholp. Although we do not know the reason for this discrepancy, the punctate staining pattern of Rholp observed by McCaffrey et al. (1991) might be due to cross-reaction of the polyclonal anti-Rholp antibody with Rholp-like protein, such as Cdc42p, Rho2p, Rho3p, or Rho4p. In mammalian cells, it has been

demonstrated that RhoA is present in the both cytosolic and particulate fractions as in yeast cells, and immunofluorescence microscopy has revealed that RhoA is present in the cytoplasm and that no particular intracellular regions have been stained (Adamson et al., 1992). Further detailed studies are required to know whether RhoA is present in any particular intracellular space(s).

Western blot analysis demonstrated that ~70 and 30% of HA-Rholps were present in the 100,000 *g* cytosolic fraction and in the particulate fraction, respectively. In mammalian cells, the cytosolic RhoA has been found to be complexed with *Rho* GDI, which is a GDI for GTP-binding proteins of the Rho family including RhoA (Kuroda et al., 1992; Regazzi et al., 1992). Thus, we presume that the cytosolic Rholp may be complexed with a counterpart of *Rho* GDI in yeast. In fact, we have recently found that there is a substantial *Rho* GDI-like activity in the cytosolic fraction of yeast cells (T. Masuda, K. Tanaka, H. Nonaka, W. Yamochi, A. Maeda, and Y. Takai, manuscript in preparation). If the cytosolic Rholp is complexed with *Rho* GDI, it might be in the GDP-bound form, since *Rho* GDI preferentially interacts with the GDP-bound form of Rho proteins (Hori et al., 1991; Mizuno et al., 1991; Takai et al., 1992). On the contrary, Rholp localized at the sites of cell growth should be in the GTP-bound form, since it is well established that small G proteins are active in the GTP-bound form and are inactive in the GDP-bound form. It may be noted that McCaffrey et al. (1991) has reported that ~20 and 80% of Rholps are present in the 100,000 *g* cytosolic fraction and in the particulate fraction, respectively. This result is inconsistent with our result that HA-Rholp was mostly present in the cytosolic fraction. The exact reason for the discrepancy between their and our results is not known at present, but our result is more likely because of the following two reasons: (*a*) we have previously shown that the substantial amount of RhoA is present in the cytosolic fraction in a complex with *Rho* GDI in bovine aortic smooth muscle (Kawahara et al., 1990; Kuroda et al., 1992); and (*b*) McCaffrey et al. (1991) have quantitated Rholp by measuring the ADP-ribosylation of Rholp. We have previously shown that the ADP-ribosylation of RhoA is inhibited by *Rho* GDI, which is present in the cytosolic fraction in a complex with RhoA (Kikuchi et al., 1992). Therefore, McCaffrey et al. (1991) might underestimate the amount of cytosolic Rholp.

It has not been clarified to which protein Rholp is bound at the sites of cell growth. This protein, which might be a target protein of Rholp, was clearly limited in amount since overexpressed Rholp was nonspecifically localized to the periphery of cells. How is Rholp localized to the sites of cell growth? We presume that Cdc42p may play a crucial role in this process. A temperature-sensitive mutant defective in the *CDC42* gene is unable to bud at restrictive temperatures, but continues growth and the nuclear cycle of DNA synthesis and nuclear division (Adams et al., 1990; Johnson and Pringle, 1990). Thus, this *cdc42* mutant arrests development as large, unbudded cells that often contain two or more nuclei. Consistently, staining of *cdc42* mutant cells with rhodamine phalloidin results in an uniform distribution of cortical actin patches (Adams et al., 1990). We stained the *cdc42* mutant cells expressing HA-Rholp with 12CA5 mAb and found that HA-Rholp was not localized to any specific site of arrested cells (data not shown). Therefore, Cdc42p appears to regulate the localization of Rholp or the Rholp-binding protein.

Based on the results of immunofluorescence microscopy of Rholp and of phenotypic analysis of the *rhol-104* mutant, we presume that Rholp plays an important role, directly or indirectly, in the process of localized cell growth, including vesicle fusion to the plasma membrane or cell wall growth at the bud tips. Since cell polarity was established in the arrested *rhol* mutant cells, Rholp seemed to function downstream of Cdc42p. Another phenotypic difference between *cdc42* and *rhol* mutants was that *rhol* mutants halted cell growth under the restrictive conditions, probably due to cell death. A possible cause for cell death may be lysis of the *rhol* mutant cells, whose molecular mechanism remains to be elucidated. Rholp was also stained in cells prior to or during cytokinesis. In these cells, staining was observed at the plasma membrane region at the mother–bud neck, where cortical actin patches were also concentrated. This result may suggest that Rholp plays a role in localized cell growth accompanying cytokinesis. In accordance with this, we have recently shown that the microinjection of C_3 or *Rho* GDI inhibits the cytokinesis in *Xenopus* embryo (Kishi et al., 1993). However, the *rhol-104* cells arrested at nonpermissive temperature did not accumulate cells with large buds. Further investigations are needed with respect to the role of Rholp in cytokinesis.

Suppression of the *rhol-104* mutation by the expression of *Rho*A suggests that the function of *Rho*A is conserved in lower eukaryotes such as yeast. Although the precise mechanism has not been established yet, *Rho*A has been proposed to be involved in the reorganization of actin stress fibers in mammalian cells (Ridley and Hall, 1992). The GTP-bound form of RhoA rapidly stimulates the stress fiber and focal adhesion formation when microinjected into serum-starved Swiss 3T3 cells. Colocalization of Rholp with cortical actin patches raises a possibility that the function of Rholp is also somehow concerned with the actin cytoskeleton system in yeast. Although cortical actin patches were concentrated to tiny or small buds in the *rhol-104* cells arrested at nonpermissive temperatures, it remains possible that Rholp is involved in the reorganization of the actin system after the cell polarity has been established. Identification of genes functionally interacting with *RHO1* may reveal a relationship between *RHO1* and the actin cytoskeleton system.

We thank Pascal Madaule for providing a plasmid pWT and yeast strain MM50, Fuyu Tamanoi for advice on the HA epitope addition method, Kenji Irie for performing the flow cytometric analysis on the *rho1* mutants, Shoichiro Tsukita for valuable comments, and Yoshikazu Ohya and Hiroshi Qadota for fruitful discussions, providing a plasmid YEpT-RHO1, and communicating the unpublished results before publication.

This investigation was supported by Grants-in-Aid for Scientific Research and for Cancer Research from the Ministry of Education, Science, and Culture, Japan (1992, 1993), by Grants-in-Aid for Abnormalities in Hormone Receptor Mechanisms and for Aging and Health from the Ministry of Health and Welfare, Japan (1992, 1993), and by grants from the Human Frontier Science Program (1992) and the Yamanouchi Foundation for Research on Metabolic Disease (1992, 1993).

Received for publication 17 September 1993 and in revised form 31 January 1994.

References

Adams, A. E. M., and J. R. Pringle. 1984. Relationship of actin and tubulin distribution to bud growth in wild-type and morphogenetic-mutant *Saccharomyces cerevisiae*. *J. Cell Biol.* 98:934–945.

Adams, A. E. M., and J. R. Pringle. 1991. Staining of actin with fluorochrome-conjugated phalloidin. *Methods Enzymol.* 194:729–731.

Adams, A. E. M., D. I. Johnson, R. M. Longnecker, B. F. Sloat, and J. R. Pringle. 1990. *CDC42* and *CDC43*, two additional genes involved in budding and the establishment of cell polarity in the yeast *Saccharomyces cerevisiae*. *J. Cell Biol.* 111:131–142.

Adamson, P., H. F. Paterson, and A. Hall. 1992. Intracellular localization of the $P21^{rho}$ proteins. *J. Cell Biol.* 119:617–627.

Aktories, K., S. Rösener, U. Blaschke, and G. S. Chhatwal. 1988. Botulinum ADP-ribosyltransferase C3: purification of the enzyme and characterization of the ADP-ribosylation reaction in platelet membranes. *Eu. J. Biochem.* 172:445–450.

Ando, S., K. Kaibuchi, T. Sasaki, K. Hiraoka, T. Nishiyama, T. Mizuno, M. Asada, H. Nunoi, I. Matsuda, Y. Matsuura, P. Polakis, F. McCormick, and Y. Takai. 1992. Post-translational processing of *rac* p21s is important both for their interaction with the GDP/GTP exchange proteins and for their activation of NADPH oxidase. *J. Biol. Chem.* 267:25709–25713.

Boeke, J. D., F. LaCroute, and G. R. Fink. 1984. A positive selection for mutants lacking orotidine-5'-phosphate decarboxylase activity in yeast: 5-fluoro-orotic acid resistance. *Mol. Gen. Genet.* 197:345–346.

Bourne, H. R., D. A. Sanders, and F. McCormick. 1991. The GTPase superfamily: conserved structure and molecular mechanism. *Nature (Lond.).* 349:117–127.

Drubin, D. G. 1991. Development of cell polarity in budding yeast. *Cell.* 65:1093–1096.

Field, J., J. Nikawa, D. Broek, B. MacDonald, L. Rodgers, I. A. Wilson, R. A. Lerner, and M. Wigler. 1988. Purification of a *RAS*-responsive adenylyl cyclase complex from *Saccharomyces cerevisiae* by use of an epitope addition method. *Mol. Cell Biol.* 8:2159–2165.

Fukumoto, Y., K. Kaibuchi, Y. Hori, H. Fujioka, S. Araki, T. Ueda, A. Kikuchi, and Y. Takai. 1990. Molecular cloning and characterization of a novel type of regulatory protein (GDI) for the *rho* proteins, *ras* p21-like small GTP-binding proteins. *Oncogene.* 5:1321–1328.

Gietz, D., A. S. Jean, R. A. Woods, and R. H. Schiestl. 1992. Improved method for high efficiency transformation of intact yeast cells. *Nucleic Acids Res.* 20:1425.

Hall, A. 1990. The cellular functions of small GTP-binding proteins. *Science (Wash. DC).* 249:635–640.

Hart, M. J., A. Eva, T. Evans, S. A. Aaronson, and R. A. Cerione. 1991. Catalysis of guanine nucleotide exchange on the CDC42Hs protein by the *dbl* oncogene product. *Nature (Lond.).* 354:311–314.

Hartwell, L. H. 1971. Genetic control of the cell division cycle in yeast: IV. Genes controlling bud emergence and cytokinesis. *Exp. Cell Res.* 69:265–276.

Hartwell, L. H., J. Culotti, J. R. Pringle, and B. J. Reid. 1974. Genetic control of the cell division cycle in yeast. *Science (Wash. DC).* 183:46–51.

Higuchi, R. 1989. Using PCR to engineer DNA. *In* PCR Technology. H. A. Erlich, editor. Macmillan Publishers Ltd., United Kingdom. 61–70.

Hill, J. E., A. M. Myers, T. J. Koerner, and A. Tzagoloff. 1986. Yeast *E. coli* shuttle vectors with multiple unique restriction sites. *Yeast.* 2:163–167.

Hirata, K., A. Kikuchi, T. Sasaki, S. Kuroda, K. Kaibuchi, Y. Matsuura, H. Seki, K. Saida, and Y. Takai. 1992. Involvement of *rho* p21 in the GTP-enhanced calcium ion sensitivity of smooth muscle contraction. *J. Biol. Chem.* 267:8719–8722.

Hori, Y., A. Kikuchi, M. Isomura, M. Katayama, Y. Miura, H. Fujioka, K. Kaibuchi, and Y. Takai. 1991. Post-translational modifications of the C-terminal region of the *rho* protein are important for its interaction with membranes and the stimulatory and inhibitory GDP/GTP exchange proteins. *Oncogene.* 6:515–522.

Horiuchi, H., K. Kaibuchi, M. Kawamura, Y. Matsuura, N. Suzuki, Y. Kuroda, T. Kataoka, and Y. Takai. 1992. The posttranslational processing of *ras* p21 is critical for its stimulation of yeast adenylate cyclase. *Mol. Cell Biol.* 12:4515–4520.

Isomura, M., K. Kaibuchi, T. Yamamoto, S. Kawamura, M. Katayama, and Y. Takai. 1990. Partial purification and characterization of GDP dissociation stimulator (GDS) for the *rho* proteins from bovine brain cytosol. *Biochem. Biophys. Res. Commun.* 169:652–659.

Ito, H., Y. Fukuda, K. Murata, and A. Kimura. 1983. Transformation of intact yeast cells treated with alkali cations. *J. Bacteriol.* 153:163–168.

Itoh, T., K. Kaibuchi, T. Masuda, T. Yamamoto, Y. Matsuura, A. Maeda, K. Shimizu, and Y. Takai. 1993. The post-translational processing of *ras* p21 is critical for its stimulation of mitogen-activated protein kinase. *J. Biol. Chem.* 268:3025–3028.

Johnson, D. I., and J. R. Pringle. 1990. Molecular characterization of *CDC42*, a *Saccharomyces cerevisiae* gene involved in the development of cell polarity. *J. Cell Biol.* 111:143–152.

Kaibuchi, K., T. Mizuno, H. Fujioka, T. Yamamoto, K. Kishi, Y. Fukumoto, Y. Hori, and Y. Takai. 1991. Molecular cloning of the cDNA for stimulatory GDP/GTP exchange protein for *smg* p21s (*ras* p21-like small GTP-binding proteins) and characterization of stimulatory GDP/GTP exchange protein. *Mol. Cell Biol.* 11:2873–2880.

Katayama, M., M. Kawata, Y. Yoshida, H. Horiuchi, T. Yamamoto, Y. Matsuura, and Y. Takai. 1991. The posttranslationally modified C-terminal structure of bovine aortic smooth muscle *rho*A p21. *J. Biol. Chem.* 266: 12639–12645.

Kawahara, Y., M. Kawata, M. Sunako, S. Araki, M. Koide, T. Tsuda, H. Fukuzaki, and Y. Takai. 1990. Identification of a major GTP-binding protein in bovine aortic smooth muscle cytosol as the *rho*A gene product. *Biochem. Biophys. Res. Commun.* 170:673–683.

Kikuchi, A., K. Yamamoto, T. Fujita, and Y. Takai. 1988. ADP-ribosylation of the bovine brain *rho* protein by botulinum toxin type C1. *J. Biol. Chem.* 263:16303–16308.

Kikuchi. A., S. Kuroda, T. Sasaki, K. Kotani, K. Hirata, M. Katayama, and Y. Takai. 1992. Functional interactions of stimulatory and inhibitory GDP/GTP exchange proteins and their common substrate small GTP-binding protein. *J. Biol. Chem.* 267:14611–14615.

Kilmartin, J. V., and A. E. M. Adams. 1984. Structural rearrangements of tubulin and actin during the cell cycle of the yeast *Saccharomyces*. *J. Cell Biol.* 98:922–933.

Kishi, K., T. Sasaki, S. Kuroda, T. Itoh, and Y. Takai. 1993. Regulation of cytoplasmic division of *Xenopus* embryo by *rho* p21 and its inhibitory GDP/GTP exchange protein (*rho* GDI). *J. Cell Biol.* 120:1187–1195.

Kolodziej, P. A., and R. A. Young. 1991. Epitope tagging and protein surveillance. *Methods Enzymol.* 194:508–519.

Kuchler, K., H. G. Dohlman, and J. Thorner. 1993. The a-factor transporter (*STE6* gene product) and cell polarity in the yeast *Saccharomyces cerevisiae*. *J. Cell Biol.* 120:1203–1215.

Kuroda, S., A. Kikuchi, K. Hirata, T. Masuda, K. Kishi, T. Sasaki, and Y. Takai. 1992. Cooperative function of *rho* GDS and *rho* GDI to regulate *rho* p21 activation in smooth muscle. *Biochem. Biophys. Res. Commun.* 185:473–480.

Lang, P., L. Guizani, I. Vitté-Mony, R. Stancou, O. Dorseuil, G. Gacon, and J. Bertoglio. 1992. ADP-ribosylation of the *ras* related, GTP-binding protein RhoA inhibits lymphocyte-mediated cytotoxicity. *J. Biol. Chem.* 267: 11677–11680.

Lee, K. S., L. K. Hines, and D. E. Levin. 1993. A pair of functionally redundant yeast genes (*PPZ1* and *PPZ2*) encoding type 1-related protein phosphatases function within the *PKC1*-mediated pathway. *Mol. Cell Biol.* 13: 5843–5853.

Lelias, J.-M., C. N. Adra, G. M. Wulf, J.-C. Guillemot, M. Khagad, D. Caput, and B. Lim. 1993. cDNA cloning of a human mRNA preferentially expressed in hematopoietic cells and with homology to a GDP-dissociation inhibitor for the rho GTP-binding proteins. *Proc. Natl. Acad. Sci. USA.* 90:1479–1483.

Levin, D. E., and E. Bartlett-Heubusch. 1992. Mutants in the *S. cerevisiae* *PKC1* gene display a cell cycle-specific osmotic stability defect. *J. Cell Biol.* 116:1221–1229.

Madaule, P., R. Axel, and A. M. Myers. 1987. Characterization of two members of the *rho* gene family from the yeast *Saccharomyces cerevisiae*. *Proc. Natl. Acad. Sci. USA.* 84:779–783.

Matsui, Y., and A. Toh-e. 1992. Yeast *RHO3* and *RHO4* ras super-family genes are necessary for bud growth, and their defect is suppressed by a high dose of bud formation genes *CDC42* and *BEM1*. *Mol. Cell Biol.* 12:5690–5699.

McCaffrey, M., J. S. Johnson, B. Goud, A. M. Myers, J. Rossier, M. R. Popoff, P. Madaule, and P. Boquet. 1991. The small GTP-binding protein Rho1p is localized on the Golgi apparatus and post-Golgi vesicles in *Saccharomyces cerevisiae*. *J. Cell Biol.* 115:309–319.

Miura, Y., A. Kikuchi, T. Musha, S. Kuroda, H. Yaku, T. Sasaki, and Y. Takai. 1993. Regulation of morphology by *rho* p21 and its inhibitory GDP/GTP exchange protein (*rho* GDI) in Swiss 3T3 cells. *J. Biol. Chem.* 268:510–515.

Mizuno, T., K. Kaibuchi, T. Yamamoto, M. Kawamura, T. Sakoda, H. Fujioka, Y. Matsuura, and Y. Takai. 1991. A stimulatory GDP/GTP exchange protein for smg p21 is active on the post-translationally processed form of c-Ki-ras p21 and rhoA p21. *Proc. Natl. Acad. Sci. USA.* 88: 6442–6446.

Morii, N., T. Teru-uchi, T. Tominaga, N. Kumagai, S. Kozaki, F. Ushikubi, and S. Narumiya. 1992. A *rho* gene product in human blood platelets: II. effects of the ADP-ribosylation by botulinum C3 ADP-ribosyltransferase on platelet aggregation. *J. Biol. Chem.* 267:20921–20926.

Narumiya, S., A. Sekine, and M. Fujiwara. 1988. Substrate for botulinum ADP-ribosyltransferase, Gb, has an amino acid sequence homologous to a putative *rho* gene product. *J. Biol. Chem.* 263:17255–17257.

Nelson, W. J. 1992. Regulation of cell surface polarity from bacteria to mammals. *Science (Wash. DC).* 258:948–955.

Ninomiya-Tsuji, J., S. Nomoto, H. Yasuda, S. I. Reed, and K. Matsumoto. 1991. Cloning of a human cDNA encoding a CDC2-related kinase by complementation of a budding yeast *cdc28* mutation. *Proc. Natl. Acad. Sci. USA.* 88:9006–9010.

Nishiyama, T., T. Sasaki, K. Takaishi, M. Kato, H. Yaku, K. Araki, Y. Matsuura, and Y. Takai. 1994. *rac* p21 is involved in insulin-induced membrane ruffling and *rho* p21 is involved in hepatocyte growth factor- and 12-O-tetrade-canoylphorbol-13-acetate (TPA)-induced membrane ruffling in KB cells. *Mol. Cell Biol.* 14:2447–2456.

Novick, P., and D. Botstein. 1985. Phenotypic analysis of temperature-sensitive yeast actin mutants. *Cell.* 40:405–416.

Paravicini, G., M. Cooper, L. Friedli, D. J. Smith, J.-L. Carpentier, L. S. Klig, and M. A. Payton. 1992. The osmotic integrity of the yeast cell requires a functional *PKC1* gene product. *Mol. Cell Biol.* 12:4896–4905.

Paterson, H. F., A. J. Self, M. D. Garrett, I. Just, K. Aktories, and A. Hall.

1990. Microinjection of recombinant p21^{rho} induces rapid changes in cell morphology. *J. Cell Biol.* 111:1001–1007.

Pringle, J. R., and L. H. Hartwell. 1981. The *Saccharomyces cerevisiae* cell cycle. *In* The Molecular Biology of the Yeast *Saccharomyces*. J. D. Strathern, E. W. Jones, and J. R. Broach, editors. Cold Spring Harbor Laboratory, Cold Spring Harbor, New York. 97–142.

Pringle, J. R., A. E. M. Adams, D. G. Drubin, and B. K. Haarer. 1991. Immunofluorescence methods for yeast. *Methods Enzymol.* 194:565–602.

Qadota, H., I. Ishii, A. Fujiyama, Y. Ohya, and Y. Anraku. 1992. *RHO* gene products, putative small GTP-binding proteins, are important for activation of the *CAL1/CDC43* gene product, a protein geranylgeranyltransferase in *Saccharomyces cerevisiae*. *Yeast.* 8:735–741.

Regazzi, R., A. Kikuchi, Y. Takai, and C. B. Wollheim. 1992. The small GTP-binding proteins in the cytosol of insulin-secreting cells are complexed to GDP dissociation inhibitor proteins. *J. Biol. Chem.* 267:17512–17519.

Ridley, A. J., and A. Hall. 1992. The small GTP-binding protein rho regulates the assembly of focal adhesions and actin stress fibers in response to growth factors. *Cell.* 70:389–399.

Rose, M. D., and G. R. Fink. 1987. *KAR1*, a gene required for function of both intranuclear and extranuclear microtubules in yeast. *Cell.* 48:1047–1060.

Rothstein, R. 1991. Targeting, disruption, replacement, and allele rescue: integrative DNA transformation in yeast. *Methods Enzymol.* 194:281–301.

Rubin, E. J., D. M. Gill, P. Boquet, and M. R. Popoff. 1988. Functional modification of a 21-kilodalton G protein when ADP-ribosylated by exoenzyme C3 of *Clostridium botulinum*. *Mol. Cell Biol.* 8:418–426.

Sambrook, J., E. F. Fritsch, and T. Maniatis. 1989. Molecular Cloning: A Laboratory Manual. Cold Spring Harbor Laboratory, Cold Spring Harbor, New York. 545 pp.

Sherman, F., G. R. Fink, and J. B. Hicks. 1986. Methods in Yeast Genetics. Cold Spring Harbor Laboratory, Cold Spring Harbor, New York. 186 pp.

Sikorski, R. S., and P. Hieter. 1989. A system of shuttle vectors and yeast host strains designed for efficient manipulation of DNA in *Saccharomyces cerevisiae*. *Genetics.* 122;19–27.

Sikorski, R. S., and J. D. Boeke. 1991. *In vitro* mutagenesis and plasmid shuffling: from cloned gene to mutant yeast. *Methods Enzymol.* 194: 302–318.

Sloat, B. F., A. Adams, and J. R. Pringle. 1981. Roles of the *CDC24* gene product in cellular morphogenesis during the *Saccharomyces cerevisiae* cell cycle. *J. Cell Biol.* 89:395–405.

Takai, Y., K. Kaibuchi, A. Kikuchi, and M. Kawata. 1992. Small GTP-binding proteins. *Int. Rev. Cytol.* 133:187–230.

Takaishi, K., A. Kikuchi, S. Kuroda, K. Kotani, T. Sasaki, and Y. Takai. 1993. Involvement of *rho* p21 and its inhibitory GDP/GTP exchange protein (*rho* GDI) in cell motility. *Mol. Cell Biol.* 13:72–79.

Takaishi, K., T. Sasaki, M. Kato, W. Yamochi, S. Kuroda, T. Nakamura, M. Takeichi, and Y. Takai. 1994. Involvement of *Rho* p21 small GTP-binding protein and its regulator in the HGF-induced cell motility. *Oncogene.* 9:273–279.

Tominaga, T., K. Sugie, M. Hirata, N. Morii, J. Fukata, A. Uchida, H. Imura, and S. Narumiya. 1993. Inhibition of PMA-induced, LFA-1–dependent lymphocyte aggregation by ADP ribosylation of the small moelcular weight GTP binding protein, *rho*. *J. Cell Biol.* 120:1529–1537.

Valencia, A., P. Chardin, A. Wittinghofer, and C. Sander. 1991. The *ras* protein family: evolutionary tree and role of conserved amino acids. *Biochemistry.* 30:4637–4648.

Wilson, I. A., H. L. Niman, R. A. Houghten, A. R. Cherenson, M. L. Connolly, and R. A. Lerner. 1984. The structure of an antigenic determinant in a protein. *Cell.* 37:767–778.

Yaku, H., T. Sasaki, and Y. Takai. 1994. The *Dbl* oncogene product as a GDP/GTP exchange protein for the *Rho* family: its properties in comparison with those of *Smg* GDS. *Biochem. Biophys. Res. Commun.* 198:811–817.